Mask bias in submicron optical lithography

Chris A. Mack and Patricia M. Kaufman
Department of Defense, Fort Meade, Maryland 20755

(Received 16 June 1988; accepted 25 August 1988)

The effects of mask bias on the performance of an optical lithographic process are examined theoretically and experimentally. By studying the effects of bias on the aerial image, the fundamental reasons for process improvement with bias are made clear. Simulations are used to examine mask linearity and exposure and focus latitude as a function of bias. Experimental data confirm the improvement in latitude for isolated lines with bias. The proximity effect is investigated and shown to be not well understood. Two possible explanations for the proximity effect, image flare and developer depletion, are studied.

I. INTRODUCTION

As optical lithography enters the submicron regime, the ability to match photoresist feature size with the mask dimension over a wide range of mask configurations with good process latitude becomes an impossible goal. It has been observed that mask biasing can improve the performance of a lithographic process. In general, mask bias means printing a particular feature size using a mask of a slightly different size. For positive photoresists, mask bias increases the mask dimensions of the lines and decreases the mask dimensions of the spaces. Overexposure is then used to give the proper linewidth on the wafer.

The reasons for biasing are many and are the result of the fundamental properties of the aerial image. Thus, any study of mask bias effects must begin with an analysis of the effects of biasing on the aerial image. Using the log-slope technique introduced previously,[1] the effect of bias on resolution and depth-of-focus can be determined under a variety of conditions (e.g., feature size or type) by examining the aerial image.

Using primary parameter simulation techniques (such as the program PROLITH[2]), further effects of biasing can be studied. Exposure penalty, mask linearity, and exposure and focus latitude can all be investigated using PROLITH. This analysis, along with the log-slope technique, enables one to draw several general conclusions about biasing and how to effectively employ mask bias for improved lithographic performance. Experimental data are used to confirm the conclusions made using simulations.

Biasing has also been used as a proximity correction technique. The linewidth of a small isolated feature can be quite different from a dense feature (e.g., equal lines and spaces) of nominally the same size. If this dependence of linewidth on the proximity of other features is known, the mask can be adjusted accordingly.

Simple biasing techniques do not vary the amount of bias with feature size and do not take into account proximity effects. Currently, mask layout tools are available which have the sophistication necessary to adjust the bias to account for proximity and feature size effects. What is needed is a simple and accurate technique for determining the optimum bias conditions for a variety of mask configurations. This study, which looks at the fundamental reasons for mask bias as well as the nature of the proximity effect, is a first step in achieving this goal.

II. AERIAL IMAGE

Many of the effects of mask biasing can be determined by studying its effect on the aerial image. The aerial image can be best studied by understanding the nature of the interaction of the image with the photoresist process. A previous study[3] has characterized the effects of the aerial image on the photoresist with the following general results. An aerial image $I(x)$ exposes the photoresist to produce some chemical distribution $m(x)$ within the resist, x being the horizontal direction. This distribution is called the latent image. Many important properties of the lithographic process, such as exposure and development latitude, are a function of the gradient of the latent image $\partial m/\partial x$. Larger gradients result in improved process latitude. It has been shown that the latent image gradient is related to the aerial image by[3]

$$\frac{\partial m}{\partial x} \propto \frac{\partial \ln I}{\partial x}. \tag{1}$$

The development properties of the photoresist translate the latent image gradient into a development gradient, which then allows for the generation of a photoresist image. Optimum photoresist image quality is obtained with a large development rate gradient. A lumped parameter called the photoresist contrast γ can be defined which relates the aerial image and the development rate r (Ref. 3):

$$\frac{\partial \ln r}{\partial x} = \gamma \frac{\partial \ln I}{\partial x}. \tag{2}$$

The development rate gradient is maximized by higher resist contrast and by a larger slope of the log-aerial image (the log slope).

The effects of focus on a lithographic process can be characterized by a graph of the log slope versus defocus.[1] Consider the aerial images shown in Fig. 1(a) for different focus conditions. One important effect of defocus is a reduction of the slope of the image near the nominal line edge. Figure 1(b) shows the log slope of these images. One can see that defocus results in a decrease in the log slope. It is interesting to note that the log slope varies considerably with horizontal position x. The position of interest with respect to lithogra-

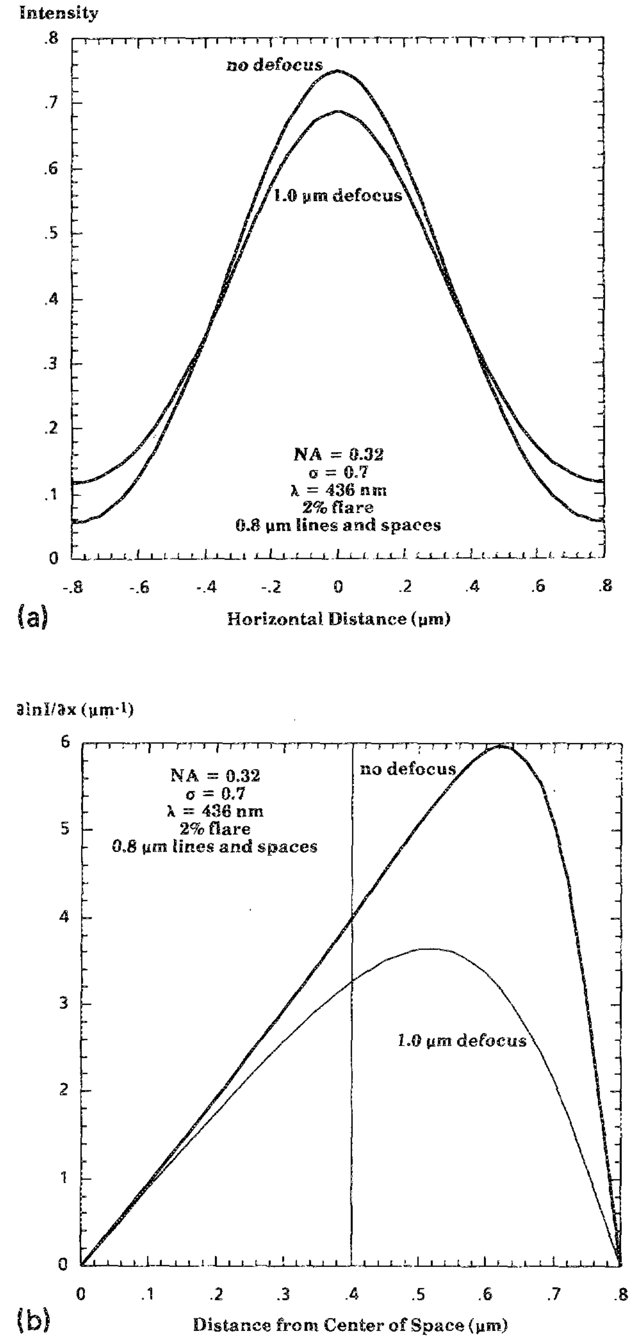

FIG. 1. The effect of defocus on the aerial image: (a) in focus and 1.0-μm defocused aerial images were predicted using PROLITH, and (b) variation of the slope of the log image with horizontal position (the mask edge is represented by the vertical line).

phic performance is the nominal line edge. For the case of no mask bias, the line edge is the same as the mask edge and is shown in Fig. 1(b) by the solid vertical line at $x = 0.4\ \mu$m. Interestingly, the maximum value of the log slope occurs to the dark side of the mask edge. For a biased image, the desired line edge is always on the dark side of the mask edge. This points out the fundamental reason for improved lithographic performance with mask bias: a biased image has a larger value of the log slope at the line edge.

The log-slope defocus curve can now be used to study the effects of bias on resolution and depth-of-focus. Consider a 0.8-μm isolated line imaged for different amounts of mask bias. A graph of the log slope of the aerial image at the line edge versus defocus is shown in Fig. 2(a). Increasing mask bias improves the log slope for all values of focus. This results in improved depth-of-focus and process latitude. Figure 2(b) shows the equivalent curves for 0.8-μm lines and spaces. Unlike the case of an isolated line, there is only slight improvement in the log slope of equal lines and spaces with bias. Isolated spaces show results similar to the equal lines and spaces. Thus, for high-resolution features, only the isolated lines benefit significantly from mask biasing. The rea-

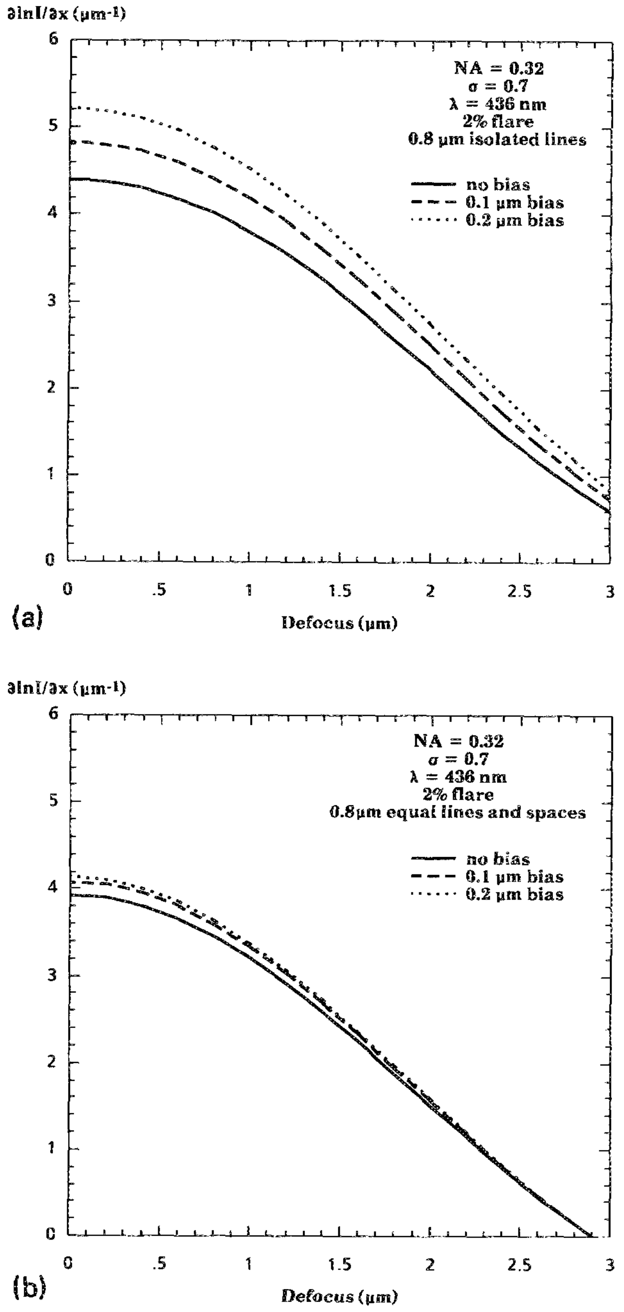

FIG. 2. The effect of bias on the depth-of-focus (using the log slope of the aerial image as a metric) of (a) an isolated 0.8-μm line, and (b) 0.8-μm equal lines and spaces.

son for this is intuitively obvious. Biasing a space means making the dimension of the space on the mask smaller. For features near the resolution limit this will seriously degrade the aerial image, counteracting the benefits of biasing discussed above. (As will be discussed later, the performance of high-resolution equal lines and spaces is dominated by the performance of the space. Thus, small dense lines do not benefit from bias.) Biasing an isolated line, however, means that the mask dimension is larger, thus improving the aerial image quality.

III. PROLITH MODELING STUDIES

Further insight into mask biasing effects can be gained using the primary parameter model PROLITH.[2] The parameters given in Table I were used in PROLITH v1.4 to simulate isolated and packed lines of different sizes as a function of mask bias. The resist parameters were chosen to be representative of a good, high-resolution *g*-line resist. The substrate was nonreflective to eliminate standing waves. Thus, the modeling conditions could be considered ideal from a resist processing point of view. Shown in Fig. 3 are the exposure energies required to give the nominal linewidth for different bias conditions. Obviously, exposure energy increases when bias is used. Although this is normally considered a detriment from the point of view of throughput, higher exposure energies result in improved exposure gradient in the photoresist, thereby yielding improved process latitude.[3] Figure 3(a) shows that the required exposure energy for isolated lines is not a strong function of feature size. This is highly desirable and leads to good mask linearity (the ability to print accurately many different feature sizes at the same time). For equal lines and spaces, however, biasing significantly reduces mask linearity by increasing the required exposure energy of small features more than the larger ones [Figs. 3(b) and 4]. Thus, biasing is actually a detriment to imaging high-resolution lines and spaces.

TABLE I. Parameters used by PROLITH in modeling studies of bias.

Image parameters	
Wavelength	463 nm
Numerical aperture	0.32
Partial coherence	0.7
Fixed defocus	0.5 μm
Image flare	0.02
Resist system	
Resist thickness	1.0 μm
Absorption A	0.6 μm^{-1}
Absorption B	0.05 μm^{-1}
Exposure rate C	0.013 cm^2/mJ
Substrate	matched
Development parameters	
Development time	30 s
R_{max}	100 nm/s
R_{min}	1 nm/s
m_{th}	0.5
n	5

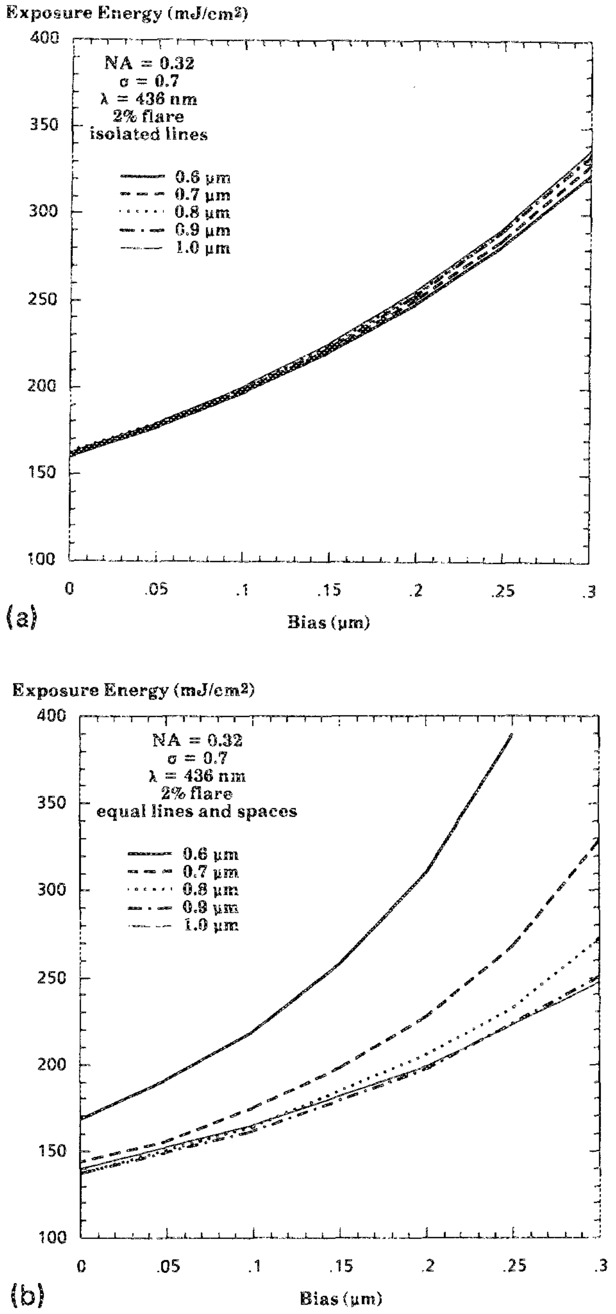

FIG. 3. The increase in exposure energy required as a function of bias for (a) isolated lines, and (b) equal lines and spaces of different sizes.

By simulating linewidth versus exposure energy, exposure latitude as a function of bias can be determined. Shown in Fig. 5(a) is the improvement in exposure latitude of isolated lines as bias is increased. Exposure latitude is defined as the percent exposure variation which gives a ± 10% linewidth change. Just as the log slope of the aerial image predicts, bias significantly improves the exposure latitude of the isolated lines. For packed lines, however, the small features do not show improvement in latitude [Fig. 5(b)], again as the log slope predicts. Larger lines and spaces do show improve-

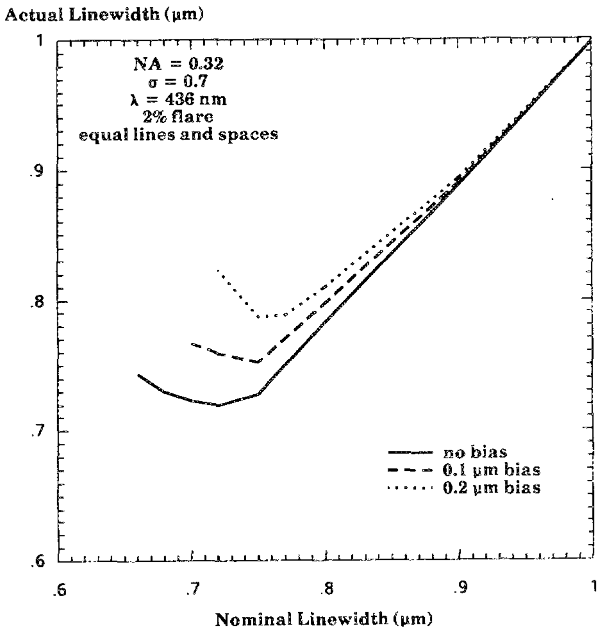

FIG. 4. Effect of mask bias on the mask linearity of equal lines and spaces (predicted by PROLITH).

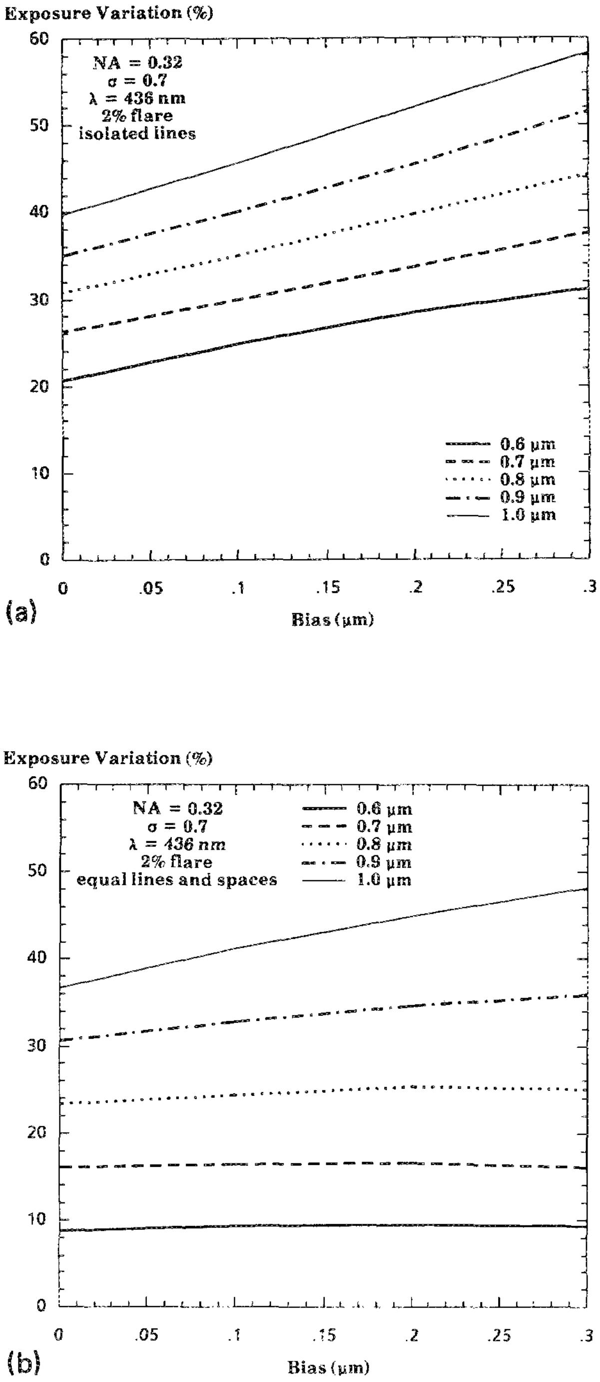

FIG. 5. The change in exposure latitude (for ± 10% linewidth variation) with bias for (a) isolated lines, and (b) equal lines and spaces.

ment in exposure latitude with bias. This points to a fundamental lithographic property: as feature sizes become large with respect to the resolution limit, they begin to behave less like features and more like isolated edges. The results of Figs. 3–5 show that equal lines and spaces smaller than ~0.75 exhibit the detrimental effects of mask biasing, whereas larger line/space features begin to show the advantages of biasing. These same simulations also showed that bias affects the resulting resist sidewall angle. Although not shown here, the trends are identical to those for exposure latitude shown in Fig. 5. Isolated lines show an improvement in sidewall angle with mask bias, as do large line/space patterns. Smaller packed lines do not show an improvement in sidewall angle.

Figures 3–5 show some of the effects of bias on isolated lines and equal lines and spaces. Although not shown, these same simulations were also performed on isolated spaces. In every case the isolated space showed behavior very similar to the line/space features. From this observation, one can conclude that the performance of equal lines and spaces is dominated by the performance of the space. Thus, studying isolated and dense lines is sufficient to characterize the performance of a lithographic process.

PROLITH can also be used to investigate focus effects of biasing. Shown in Fig. 6 are the standard linewidth versus focus versus exposure plots for 0.8-µm equal lines and spaces for no bias and 0.2 µm of mask bias. Close examination of these curves reveals very little discernable difference between the two bias conditions. This again confirms the predictions of the log slope analysis of Fig. 2(b). The case of isolated 0.8 µm lines is given in Fig. 7. The addition of bias flattens the linewidth versus focus curves considerably, resulting in improved depth-of-focus. This again confirms the log-slope predictions [Fig. 2(a)]. The improvement in both exposure and focus latitude can be seen most conveniently in the process volume plot of Fig. 8. This graph gives the exposure variation as a function of focus to give a ± 10% linewidth change. Thus, exposure and focus values which fall inside the process "window" will meet a ± 10% linewidth specification. One can see that the effect of bias on these 0.8-µm isolated lines is to increase the size of the process window.

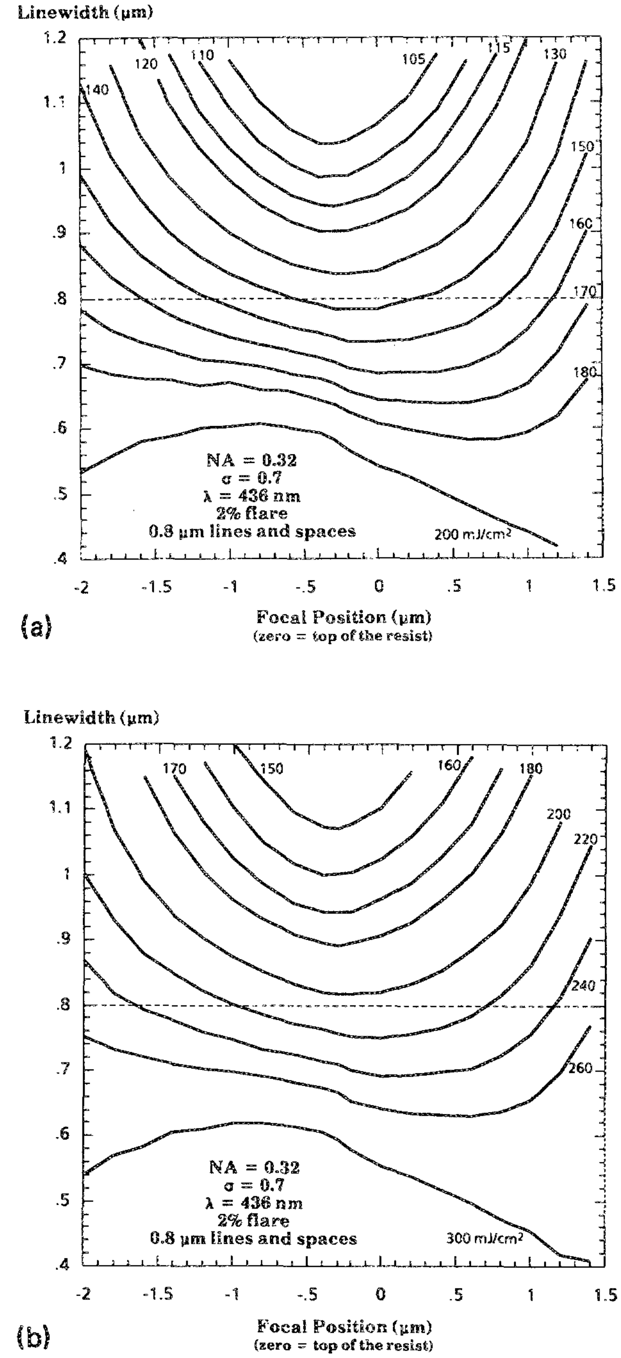

FIG. 6. Focus–exposure matrix of equal lines and spaces (simulated with PROLITH) with (a) no bias, and (b) 0.2-μm bias.

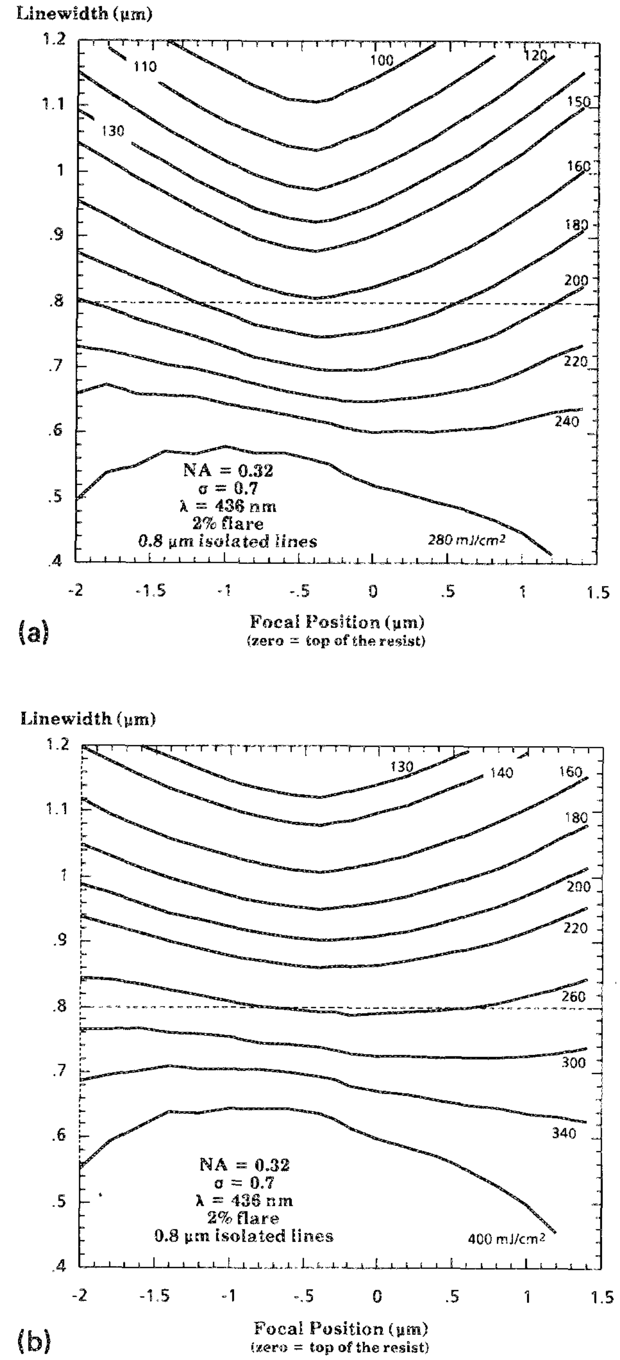

FIG. 7. Focus–exposure matrix of isolated lines (simulated with PROLITH) with (a) no bias, and (b) 0.2-μm bias.

IV. EXPERIMENTAL LINEWIDTH STUDY

In order to investigate the effects of mask biasing on linewidth, electrical linewidth measurements were performed on a variety of feature sizes and types. Silicon wafers with 1.1 kÅ of thermal oxide and 1 kÅ of aluminum were used as the substrate. After aluminum deposition, a 2-kÅ antireflective coating was spun onto the wafers, followed by a track bake. The wafers were then coated with 1.28 μm of Shipley 1400-27 photoresist and exposed on an Eaton 8605H 5:1 reduction stepper equipped with a g-line, 0.32-NA lens. After a 60-s spray development, the resist was deep-UV cured and postbaked at 130 °C. The patterned wafers were reactive ion etched and the photoresist stripped from the wafer surfaces. The final step was a sinter prior to the electrical linewidth measurements.

The linewidth data obtained from the electrical measurements resulted in plots of linewidth as a function of focal position and exposure time (i.e., focus–exposure matrices). Measurements of 1.0-μm isolated lines with and without mask bias are shown in Fig. 9. Figure 9(a) is a plot of the focus–exposure matrix of 1.0-μm lines without bias, while

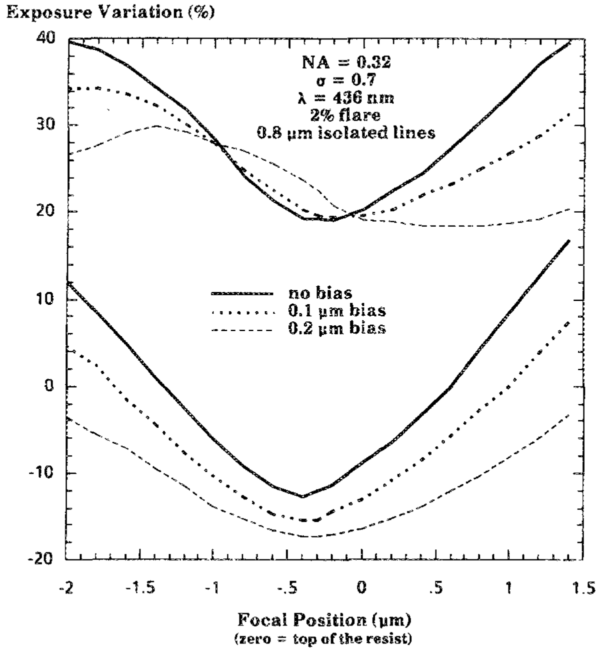

FIG. 8. Focus–exposure process volume of isolated 0.8-μm lines (simulated with PROLITH, based on a ± 10% linewidth change) for different bias amounts.

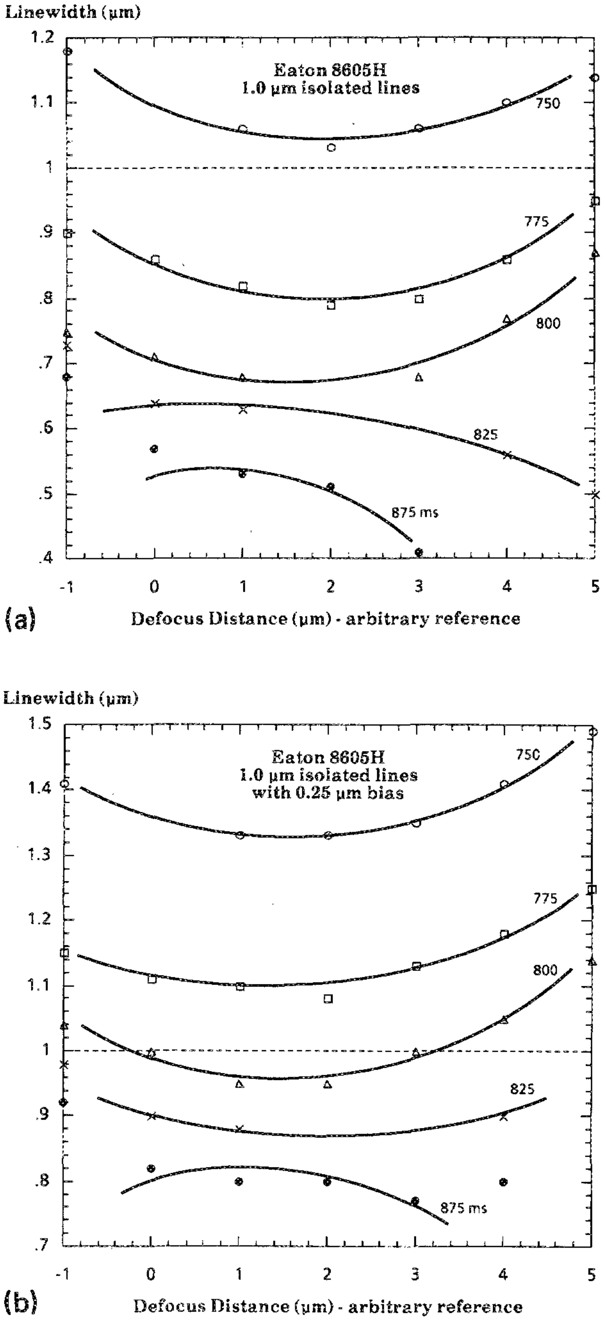

FIG. 9. Focus–exposure matrix of 1.0-μm isolated lines (experimental data) with (a) no bias, and (b) 0.25-μm bias.

Fig. 9(b) shows the same lines with 0.25-μm bias. Examining Fig. 9(a), one can see that the exposure latitude for this case is very poor. An exposure variation of just 25 ms (~3.3%) causes a linewidth change of 0.25 μm at the nominal exposure. For the biased case [Fig. 9(b)], a 25-ms change in exposure (which now corresponds to ~a 3.2% variation from the nominal) results in a 0.15-μm linewidth change. Although this exposure latitude is still not good, it is significantly better than the unbiased case.

V. PROXIMITY EFFECT

The proximity effect is defined as a change in the lithographic response of a feature (e.g., linewidth) as a function of the proximity of other nearby features. A typical example is the difference between isolated and densely packed lines. As has been shown through simulations, the exposure and focus latitude of these feature types are quite different. Further, the exposure energy required to reproduce the nominal linewidth can differ significantly between isolated and packed lines.

The electrical linewidth measurements discussed in the previous section were also used to study the proximity effect. Shown in Fig. 10 is the exposure time required to give the nominal linewidth for both isolated and packed lines of different widths. For isolated lines, there is very little dependence of exposure energy on the feature size. For the packed lines, however, smaller features require higher exposures (this is sometimes referred to as the feature size effect). Thus, if a small feature is imaged properly, the larger ones will be overexposed. Further, the packed lines require significantly more exposure than the isolated lines. Thus, if the exposure is set to reproduce the equal lines and spaces, the isolated lines will be substantially overexposed. Obviously, the proximity effect and the feature size effect are quite detrimental to a lithographic process.

Using PROLITH to simulate the proximity effect shows a dramatic discrepancy. For a partial coherence of 0.7, PROLITH predicts that the isolated lines should require slightly more energy than the densely packed lines to be properly imaged, not less (see Fig. 3). Using a variety of different resist parameters failed to alter the model's prediction. Thus, there is some phenomenon causing the observed proximity

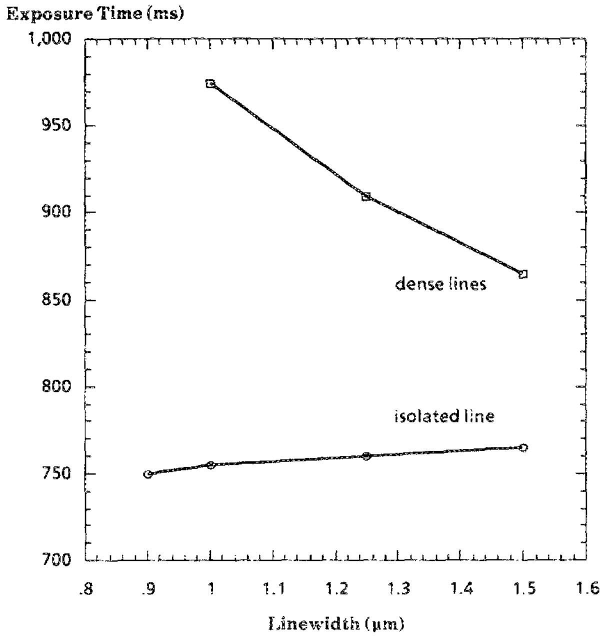

FIG. 10. Experimentally measured proximity effect—the exposure time required to give the nominal linewidth for different size isolated and dense lines.

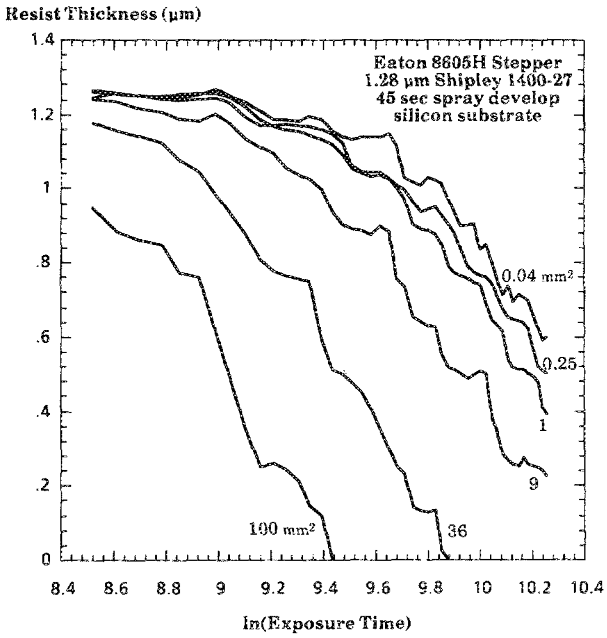

FIG. 12. Pseudo-contrast curves used to determine image flare for different die sizes.

effect which is not being taken into account by the lithography simulation package. One possibility may be a proximity-dependent image flare. Flare is an unwanted background light caused by scattering within the lens. If isolated lines exhibited significantly greater amounts of flare than packed lines, the observed proximity effect could be explained.

To investigate this possibility, the image flare was measured on the Eaton stepper used in the linewidth study. Since flare is caused by scattering of light, it seems reasonable to assume that the amount of flare is a function of the amount of light going through the lens. Thus, a bright-field mask should have more flare than a dark-field mask, and an isolated line would presumably have more flare than densely packed lines. To test this hypothesis, flare was measured as a function of the die size of a clear mask.

Flare was measured using the technique suggested by Flagello and Pomerene[4] in which photoresist is used as the detector. The exposure energy needed to just clear the photoresist in a dark area of the mask is compared to the energy needed to clear the resist in a clear area of the mask. The ratio

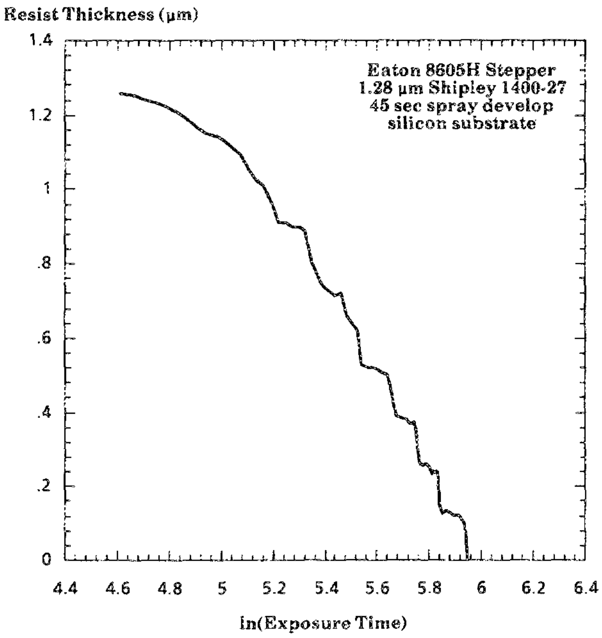

FIG. 11. Measured contrast curve used in the determination of image flare.

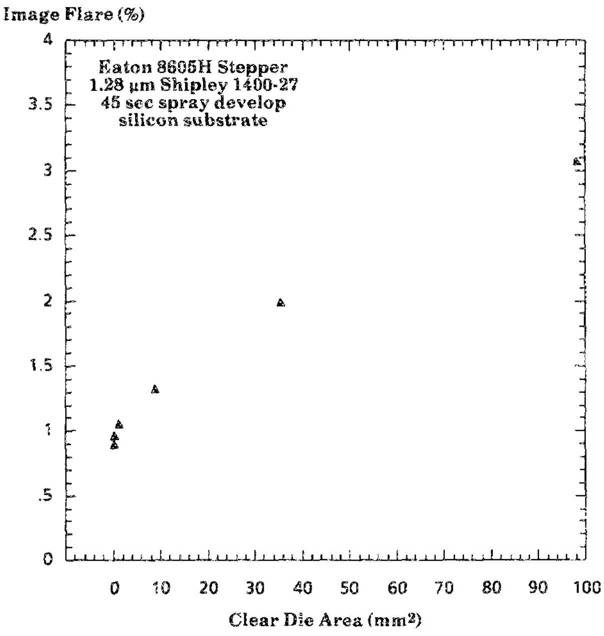

FIG. 13. Image flare as a function of die area.

of these energies is the flare. Bare silicon wafers were coated with 1.28-μm of Shipley 1400-27 positive photoresist and exposed on the Eaton 8605H reduction wafer stepper. A bright-field reticle with several large (50-μm) opaque islands was used to image the wafers, followed by a 45-s spray development. The contrast curve of the photoresist process was obtained by measuring the remaining resist thickness in the clear field area as a function of exposure and is shown in Fig. 11. This curve will serve as the basis of comparison when measuring the dark-field resist loss.

Flare was determined by measuring the thickness of the resist in the center of the 50-μm island as a function of exposure, resulting in a "pseudo-contrast" curve. This experiment was repeated for die sizes ranging from 0.04 to 100 mm^2 with the results shown in Fig. 12. It is interesting to note that the stair-step pattern due to the standing wave effect is present in the pseudo-contrast curves, indicating that the flare is indeed an image effect and not a substrate scattering effect. Comparison of the curves of Figs. 11 and 12 give the flare as a function of the clear area of the mask, shown in Fig. 13. As expected, flare is a strong function of the total amount of light passing through the lens.

Examining Fig. 13, one can see two distinct effects. First, the amount of flare rises very quickly to $\sim 1\%$ as the die size increases to 1 mm^2. This can be termed the "local" flare effect. Secondly, the amount of flare rises steadily as the die size increases, to a maximum of 3% for the 100 mm^2 die. This is a "nonlocal" flare effect which is a function of the total light passing through the lens. These data suggest that flare is definitely proximity dependent. However, one would expect the difference in flare for isolated and packed lines to be $< 1\%$, corresponding to the amount of local flare observed. Thus, this small amount of proximity dependent flare does not account for the significant proximity effects observed.

If the cause of the proximity effect is not optical, it must be due to the photoresist process. One possible explanation is developer depletion.[5] One can imagine that the flow or diffusion of developer into a small, high aspect ratio hole would be more diffcult than into a larger space, or a large clear area. If this were true, the developer in the hole would become depleted as the development continued, slowing down the development rate. Thus, small spaces would not clear as fast as large spaces, causing the observed proximity effect. Further investigation is needed to confirm this possible mechanism.

VI. CONCLUSIONS

Using simulation and experiment, several general properties of a lithographic process with mask bias were determined:

(i) The fundamental reason for improved lithographic performance with mask bias is an increase in the log slope of the aerial image at the line edge.

(ii) Isolated lines of all sizes benefit from bias. These benefits include improved exposure and focus latitude and sidewall angle.

(iii) Densely packed lines do not benefit from bias for feature sizes less than $\sim 0.75\ \lambda/\mathrm{NA}$. Larger packed lines begin to show the benefits of bias.

(iv) The performance of small packed lines and spaces is dominated by the performance of the space.

(v) Standard simulation programs fail to properly predict the proximity effect.

(vi) Although flare is proximity dependent, it cannot account for the observed proximity effect.

(vii) Developer depletion is a logical explanation for the proximity effect. Experimentation is needed to confirm this hypothesis.

Lithography modeling has proved to be a useful tool in understanding the effects of mask bias on lithographic performance. However, these models fall short of the goal of a bias optimizer for mask layout due to proximity effect discrepancies. Further work in this area may yet lead to the accomplishment of this goal.

ACKNOWLEDGMENT

The authors wish to thank David J. Mountain for setting up and performing the electrical linewidth measurements.

[1] C. A. Mack, Proc. SPIE **922**, (1988).
[2] C. A. Mack, Proc. SPIE **538**, 207 (1985).
[3] C. A. Mack, in KTI Microelectronics Seminar Interface '87 (1987) pp. 153–167.
[4] D. G. Flagello and A. T. S. Pomerene, Proc. SPIE **772**, 6 (1987).
[5] C. A. Mack, J. Electrochem. Soc. **134** (No. 1), 148 (1987).